Fitting second-order cone constraints to microbial growth data

Shuyao Tan, Emna Krichen, Alain Rapaport, Elodie Passeport, Joshua Taylor

Fitting second-order cone constraints to microbial growth data*

Shuyao Tan[a], Emna Krichen[b], Alain Rapaport[c], Elodie Passeport[a], Josh A. Taylor[d]

[a]*Department of Chemical Engineering & Applied Chemistry, University of Toronto, Canada*
[b]*Laboratoire d'Océanographie de Villefranche, CNRS UMR 7093, Sorbonne Universités, Villefranche-sur-Mer, France, France*
[c]*MISTEA, Université de Montpellier, INRAE, Institut Agro, France*
[d]*The Edward S. Rogers Sr. Department of Electrical and Computer Engineering, University of Toronto, Canada*

Abstract

Second-order cone programming is a highly tractable convex optimization class. In this paper, we fit general second-order cone constraints to data. This is of use when one must solve large-scale, nonlinear optimization problems, but modeling is either impractical or does not lead to second-order cone or otherwise tractable constraints. Our motivating application is biochemical process optimization, in which we seek to fit second-order cone constraints to microbial growth data. The fitting problem is nonconvex. We solve it using the concave-convex procedure, which takes the form of a sequence of second-order cone programs. We validate our approach on simulated and experimental microbial growth data, and compare its performance with conventional nonlinear least-squares fitting.

Keywords: Second-order cone programming, microbial growth, conic fitting, concave-convex procedure

1. Introduction

Second-order cone programming (SOCP) is a highly tractable nonlinear optimization class [1, 2]. In this paper, we fit second-order cone (SOC) constraints to data. This could be useful in several scenarios, e.g., when first principles modeling does not lead to a tractable constraint or is simply not viable, and one must solve large-scale problems that are fundamentally nonlinear.

Our motivating application is the optimization of biochemical processes, for which the Monod [3] and Contois [4] functions are established models of microbial growth. In [5], it was shown that Monod growth with constant biomass and Contois growth can be represented as SOC constraints. These models have been extensively validated over many years, but are not derived from first principles. It is therefore plausible that a general SOC constraint, which has more parameters, could accurately model a broad range of microbial growth. At the same time, by virtue of being an SOC, any such constraint could be used in an optimization problem without sacrificing tractability.

In this paper, we estimate the parameters of a general SOC constraint from data. We formulate this as an optimization problem, which is nonconvex but does have partial SOC structure. We exploit this through the concave-convex procedure (CCP) [6, 7], which here takes the form of a sequence of SOCPs. The problem nonetheless has a number of local minima and a trivial global minimum. We circumvent these difficulties using multiple starting points and by adding constraints on the parameters, as is standard in ellipse fitting [8].

To the best of our knowledge, this is the first attempt to fit general SOC constraints to data. The most relevant existing literature concerns fitting ellipses or conics to data [9, 10]. These papers often focus on problems in computer vision, and therefore in two and three dimensions. We use ideas from these papers to prohibit the trivial solution where all parameters are estimated to be zero [8], and to quantify error in terms of geometric distance [11].

There is an extensive literature on fitting microbial growth rates like the Monod and Contois functions to data [12]. The closest work to ours in this area is [13], in which splines are fit to microbial growth data. While this can better accommodate growth that does not follow a simple mathematical expression, splines are not representable as a tractable or convex constraint in an optimization problem. On the other hand, an empirically fitted SOC constraint can potentially capture a wide range of microbial growth, and is well-suited for use in large scale optimization problems arising in applications like wastewater treatment [14].

Our original contributions are as follows.

- We formulate an optimization problem for fitting SOC constraints to data. We discuss several constraints for prohibiting trivial solutions and enforcing certain practical requirements, e.g., that microbial growth is zero when the substrate or biomass is zero.
- We adapt the CCP to the optimization problem, which is implementable as a sequence of SOCPs.
- We validate our approach on three examples based on microbial growth: (i) Contois growth, which has an exact

*Funding is acknowledged from the Natural Sciences and Engineering Research Council of Canada and the French LabEx NUMEV, incorporated into the I-Site MUSE.

Brief paper

SOC representation, (ii) general Monod growth and Haldane growth, which do not have SOC representations, and (iii) experimental growth data from [15].

2. Formulation

2.1. Problem statement

We have a set of data points $z_k \in \mathbb{R}^m$, $k \in \mathcal{K}$, where $\mathcal{K}$ is an index set. We want to find the SOC constraint that best fits the data. An SOC constraint is parametrized by the matrices $A \in \mathbb{R}^{n\times m}$, $b \in \mathbb{R}^n$, $c \in \mathbb{R}^{1\times m}$, and $d \in \mathbb{R}$. Note that the number of rows in A and b, n, is a tunable parameter, which we discuss at the end of Section 3.

In standard form the SOC constraint is written

$$\|Az_k + b\| \le cz_k + d. \tag{1}$$

Note that (1) does not need to be satisfied for all $k \in \mathcal{K}$. We are rather interested in the surface on which the constraint binds, and which best goes through the data. We therefore seek to find the matrices A, b, c, and d that achieve the least squared error, given by

$$\sum_{k\in\mathcal{K}} (\|Az_k + b\| - cz_k - d)^2 .$$

Observe that there is a trivial solution wherein A, b, c, and d are all zero. To prohibit this, one or a set of the variables must be fixed at a nonzero value. For example, similar to [16], we could set $d = 1$. Because there are multiple such choices, as well as constraints representing practical requirements, we write this as the generic convex constraint $(A, b, c, d) \in \mathcal{N}$. This leads to the optimization

$$\min_{A,b,c,d} \sum_{k\in\mathcal{K}} (\|Az_k + b\| - cz_k - d)^2 \tag{2a}$$

$$\text{such that } (A, b, c, d) \in \mathcal{N}. \tag{2b}$$

We discuss the constraints that define the set $\mathcal{N}$ in more detail in Section 2.2.

If keeping the number of parameters small is also of interest, we can add a sparsity regularizer [17] to the objective such as the l_1 norm,

$$\gamma\,(|A|_1 + |b|_1 + |c|_1 + |d|)\,, \tag{2c}$$

where γ is a positive weighting factor.

In the same vein, we can choose the number of rows in A and b, n, that yields the best fit. A larger n corresponds to more parameters and a potentially more precise fit, but may lead to overfitting and increase the number of local minima.

2.2. Constraints

We now discuss the specific constraints in (2b). As mentioned in Section 2.1, there is a trivial solution in which all parameters are zero. There is a second trivial solution with one row of A equal to c and the rest zero, and there are likely more that attain zero error for any data set via perfect cancellation.

We prohibit such solutions with non-degeneracy constraints such as the following.

- The simplest such constraint is $d = 1$. However, as will be seen in Example 1, there may be good solutions with $d = 0$.
- We set the sum of the diagonal elements of A to a constant while enforcing a lower limit on each entry. This prohibits the trivial solution and is compatible with Examples 1 and 2. There is an infinite number of such linear combinations of the parameters that one could consider.
- Reference [8] uses a quadratic constraint on the parameters. Here we do not consider such constraints because they make $\mathcal{N}$ nonconvex, but note they may also be beneficial and compatible with the CCP.

There may be additional constraints arising from practical considerations. For example, one might want the fitted surface to go through zero; e.g., in Section 4, this means that there should be no microbial growth when the substrate and biomass concentrations are both zero. The corresponding constraint is obtained by requiring (1) to bind when $z = 0$:

$$\|b\| = d.$$

This is unfortunately nonconvex, but we can still make use of the convex half,

$$\|b\| \le d,$$

which is an SOC constraint. We find in the numerical examples that this does indeed force the resulting surface to go through the origin.

3. Solution via CCP

Problem (2) is a nonconvex optimization. However, given that the number of parameters will be no more than a few dozen, it is reasonable to hope for a global or good local minimum, e.g., by trying multiple starting points. We now show how to exploit the problem's partial SOC structure in the CCP [6, 7]. We also refer to [18], in which the CCP was applied to a nonlinear model of microbial growth with partial SOC structure.

We first rewrite (2) as

$$\min_{A,b,c,d} \sum_{k\in\mathcal{K}} q_k^2 \tag{3a}$$

$$\text{such that for all } k \in \mathcal{K},$$

$$\|Az_k + b\| \le q_k + cz_k + d \tag{3b}$$

$$-\|Az_k + b\| \le q_k - cz_k - d \tag{3c}$$

$$(A, b, c, d) \in \mathcal{N}. \tag{3d}$$

Here we have left out the regularizer for concision, and could add it back with no issue. Observe that (3b) is an SOC constraints and may therefore be left as is. Only (3c) is nonconvex, and must be linearized in the CCP. Let $\mathcal{J}_k(A, b)$ be the Jacobian of $-\|Az_k + b\|$.

The CCP for (3) is as follows. First, choose initial values for the parameters, A_0 and b_0, and set the iteration counter to $\alpha = 0$. Repeat the below steps until the stopping criterion has been reached.

1. Solve

$$(A_{\alpha+1}, b_{\alpha+1}) = \underset{A,b,c,d,q}{\operatorname{argmin}} \sum_{k\in\mathcal{K}} q_k^2$$

such that for all $k \in \mathcal{K}$,

$$\begin{aligned} &\|Az_k + b\| \le q_k + cz_k + d \\ &\mathcal{J}_k(A_\alpha, b_\alpha)^\top \begin{bmatrix} A - A_\alpha \\ b - b_\alpha \end{bmatrix} - \|A_\alpha z_k + b_\alpha\| \\ &\quad \le q_k - cz_k - d \\ &(A, b, c, d) \in \mathcal{N}. \end{aligned}$$

2. If the termination criterion is reached, stop. Otherwise set $\alpha = \alpha + 1$ and go to Step 1.

The termination criterion is typically the convergence of the objective and/or solution, or when α reaches a maximum number of iterations.

Based on our numerical experiments, (3) appears to possess numerous local minima. To improve the chance of finding a good solution, one can run the CCP multiple times using different values of A_0 and b_0. This is straightforward because any values of A_0 and b_0 will be feasible, and, given the offline and low-dimensional nature of the problem, the CCP generally needs no more than a second.

As a result of the nonconvexity of (3), increasing the number of rows in A and b, n, generally does not improve performance. We believe that this is because more parameters leads to more minima, making it harder to find good minima. The difficulty of finding global minima also makes it impractical to apply tools like the likelihood-ratio test to systematically choose n. In our numerical experiments, we find that $n \le m$ yields the best results.

4. Application to microbial growth

We consider a well-mixed volume with a substrate concentration, s, biomass concentration, x, and growth kinetics, r. Each data point is a measurement, $z_k = [s_k, x_k, r_k]^\top \in \mathbb{R}^3$, $k \in \mathcal{K}$. The kinetics generally take the form $r = \mu(s, x)x$, where $\mu(s, x)$ is called the growth rate. Two common cases are the Contois and Monod growth rates, which are respectively given by

$$\mu_C(s, x) = \frac{\mu^{\max} s}{K_s x + s} \quad \text{and} \quad \mu_M(s, x) = \frac{\mu^{\max} s}{K_s + s}.$$

Both are parametrized by a maximum specific growth rate, $\mu^{\max}$, and the constant, K_s [19].

The next two examples demonstrate how (2) can be used to estimate $\mu^{\max}$ and K_s for the Contois and Monod growth rates. Note, however, that we expect existing, specialized techniques to achieve better performance, and intend (2) for estimating the parameters of general SOC constraints.

Example 1 (Contois growth). *In [5], it was shown that the Contois growth constraint $r \le \mu_C(s, x)x$ is equivalent to the SOC constraint*

$$\left\| \begin{bmatrix} \mu^{\max} s \\ \mu^{\max} K_s x \\ K_s r \end{bmatrix} \right\| \le \mu^{\max} s + \mu^{\max} K_s x - K_s r.$$

We therefore want d in (1) to be zero. We normalize by setting $A_{11} = c_1 = 1$, which corresponds to dividing through by $\mu^{\max}$. The resulting parameter matrices are

$$A = \begin{bmatrix} 1 & 0 & 0 \\ 0 & K_s & 0 \\ 0 & 0 & \frac{K_s}{\mu^{\max}} \end{bmatrix}, \; c = \left[1, K_s, -\frac{K_s}{\mu^{\max}}\right].$$

We implement this in terms of (2) by setting the off-diagonal element of A to zero and enforcing the linear constraints $A_{11} = c_1 = 1$, $A_{22} = c_2$, $A_{33} = -c_3$. Given the solution to (2), the growth rate parameters are given by $K_s = A_{22}$ and $\mu^{\max} = A_{22}/A_{33}$.

Example 2 (Monod growth with constant biomass). *In [5], it was shown that if we assume the biomass is constant, i.e., $x = \bar{x}$, then the Monod growth constraint $r \le \mu_M(s, \bar{x})\bar{x}$ is equivalent to the SOC constraint*

$$\left\| \begin{bmatrix} \mu^{\max} s\bar{x} \\ K_s r \\ \mu^{\max} K_s \bar{x} \end{bmatrix} \right\| \le \mu^{\max} s\bar{x} - K_s r + \mu^{\max} K_s \bar{x}.$$

In this case, we let $z = [s, r, 1]^\top$. We normalize by setting $d = 1$, which corresponds to dividing through by $\mu^{\max} K_s \bar{x}$. The resulting parameter matrices are

$$A = \begin{bmatrix} \frac{1}{K_s} & 0 & 0 \\ 0 & \frac{1}{\mu^{\max}\bar{x}} & 0 \\ 0 & 0 & 1 \end{bmatrix}, \; c = \left[\frac{1}{K_s}, -\frac{1}{\mu^{\max}\bar{x}}, 0\right].$$

We implement this in terms of (2) by setting the off-diagonal element of A and the third entry of c to zero, and enforcing the linear constraints $A_{11} = c_1$ and $A_{22} = -c_2$. Assuming that $\bar{x}$ is known, the growth parameters are given by $K_s = 1/A_{11}$ and $\mu^{\max} = 1/(A_{22}\bar{x})$.

We remark that these are of course inequality constraints, and thus only describe the Monod or Contois kinetics when they bind. In [5] and [14], analytical conditions are given that guarantee this at the optimal solutions of certain optimizations.

4.1. Evaluation metrics

We evaluate goodness of fit in terms of the algebraic distance (AD) and geometric distance (GD) between the data and the fitted surface. Given data z_k, $k \in \mathcal{K}$, and a fitted surface with parameters (A, b, c, d), the AD is given by

$$\sum_{k\in\mathcal{K}} | \, \|Az_k + b\| - cz_k - d \, |.$$

The GD between the fitted surface and the training data is given by

$$\sum_{k\in\mathcal{K}} \min_p \|p - z_k\|^2 \quad \text{such that} \quad \|Ap + b\| - cp - d = 0.$$

GD is generally preferable to AD for fitting surfaces, but the minimization makes it difficult to compute [11]. We approximate each term in the sum by minimizing the Lagrangian

$$\min_{q_k} \|q_k - z_k\|^2 + \lambda\left(\|Aq_k + b\|^2 - (cq_k + d)^2\right), \tag{4}$$

where λ is a large positive number. This is a nonlinear program, which we solve for multiple starting points and choose the one corresponding to the lowest GD.

4.2. Numerical data generation

We used the simulation-based procedure of [13] to create substrate concentrations (s), biomass concentrations (x), and growth kinetics (r). The simulation parameters are given in Table 1.

Parameter	Value	Unit
b	0.04	1/day
K_s	3	mg/L
K_I	20	mg/L
Y	0.1	1
$\mu^{\max}$	1.6	1/day
σ_s	0.5	mg/L
σ_x	0.1	mg/L

Table 1: Simulation parameters. Note that K_s is unitless for the Contois growth rate.

The data was generated by numerically solving the system

$$\frac{ds}{dt} = -\frac{r}{Y}, \quad \frac{dx}{dt} = r - bx$$

for the Contois, Monod, and Haldane growth rates. The first two are given at the start of this section, and the Haldane kinetics by

$$r = \mu^{\max} \frac{sx}{K_s + s + s^2/K_I}.$$

Note that, unlike in Example 2, we do not assume constant biomass in any case.

The bx term accounts for the decay of the biomass, and Y is the yield. We ran the simulations for multiple initial conditions, which were chosen as follows. The initial substrate concentration ranged from 5 to 40 mg/L, at an interval of 5 mg/L; the initial biomass concentration ranged from 1 to 10 mg/L, at an interval of 1 mg/L. Together, this resulted in 80 sets of initial conditions for each growth rate. The system was solved over a nine hour period using an Euler step with a twenty minute stepsize. Samples were taken at each step, resulting in a total of 2160 data points per growth rate.

4.3. Fitting convex data—Contois growth

Here we test how well the CCP can estimate K_s and $\mu^{\max}$ when the growth rate is Contois. To enforce the structure of the Contois constraint, as described in Example 1, we include the following linear constraints in (2b) on $A \in \mathbb{R}^{3\times 3}$ and $c \in \mathbb{R}^{1\times 3}$: $A_{11} = 1$, $A_{22} > \theta$, $A_{33} > 0$, $A_{11} = c_1$, $A_{22} = c_2$, and $A_{33} = -c_3$, where θ is a positive constant. A_0 and b_0 were initialized to be all zeros. In this and the next two example, the CCP stopped when the change in the objective was less than 0.1%.

We added noise to the data according to the following four scenarios.

1. No noise.
2. Scaled zero-mean, unit-variance Gaussian noise was added to s and x after simulation. The scaling factors are σ_s and σ_x for the substrate and biomass concentrations, respectively. r was computed after adding noise.
3. Noise was added as in the previous case, but r was computed before adding noise.
4. Noise was added as in the above scenario. The growth kinetics at time t was approximated by $r(t) \approx (\ln x(t+1) - \ln x(t))x(t)/\Delta$.

The performance of CCP was compared to a Contois model fitted using the Matlab built-in function `lsqcurvefit`, which represents the standard nonlinear least squares approach. The results are summarized in Table 2.

Case	CCP	Least squares
1	GD = AD = 0	GD = AD = 0
2	GD = AD = 0	GD = 0.49, AD = 70
3	GD = 1,600, AD = 1,000	GD = 850, AD = 2,700
4	GD = 100,000, AD = 9,200	GD = 94,000, AD = 36,000

Table 2: Performance of the CCP and nonlinear least squares on Contois data. In Scenario 4, $\theta = 0.5$.

The CCP recovers $\mu^{\max}$ and K_s exactly in both Scenarios 1 and 2, while nonlinear least squares only recovers them exactly in Scenario 1. This indicates that the CCP is somewhat more robust to noise. Both models performed similarly in Scenarios 3 and 4, with CCP achieving better AD and worse GD. In Scenario 4, where the data deviates most from convexity, the CCP's performance becomes dependent on the choice of θ, and can only retrieve the correct parameters if $\theta \approx 3$. The performance of the CCP is nonetheless comparable with the standard approach in this case.

4.4. Fitting nonconvex data—Monod and Haldane growth

In this section we test how well the CCP can fit a general SOC constraint to data generated from noiseless Monod and Haldane growth kinetics, which are not concave functions. We fitted surfaces in which A and b had two rows, as we observed in other tests that additional rows did not improve accuracy. This could be due to the large number of local minima, which likely increases with the number of variables. A_0 was initialized to be all zeros and b_0 all ones.

Growth	AD	GD
Monod	0.51	52.5
Haldane	0.36	599

Table 3: Performance of the CCP on Monod and Haldane data

The results are shown in Table 3. As expected, the CCP performed better on the convex (Contois) data set than on the nonconvex (Monod and Haldane) data sets. Similarly, it attained lower error on the Monod data, which is more nearly convex, than on the Haldane data. The data and the fitted SOC surface are shown for the Monod case in Figure 1.

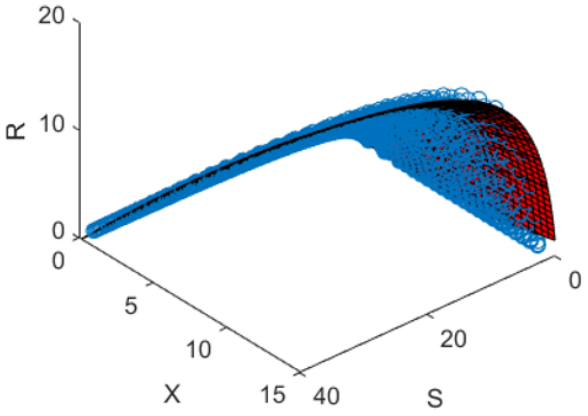

Figure 1: Plot of the fitted surface (in red) and the Monod data points (in blue).

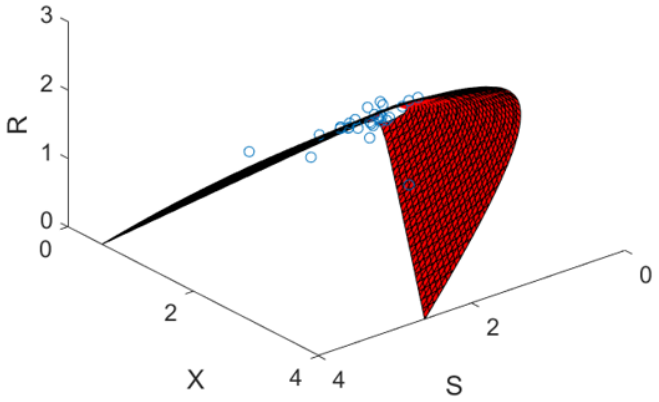

Figure 2: Plot of the fitted surface (in red) and the experimental data (in blue).

4.5. Experimental data

We lastly tested the CCP on experimental data from [20], in which biomass in a continuous biological reactor was fed diluted wine. The initial biomass concentration and the inlet substrate concentration were varied, and measurements of s and x were taken daily from days 8 to 16. The growth kinetics at time t was approximated by $r(t) \approx (\ln x(t+1) - \ln x(t))x(t)/\Delta + D$, where Δ is the sampling time interval and D is the dilution rate (1/day).

We set up the CCP as follows. The measured substrate concentrations were scaled by a factor of ten to make them commensurate with the biomass measurements. A and b have two rows. A_0 was initialized to be all zeros and b_0 all ones.

Figure 2 shows the data with the fitted surface. For each data point $k \in \mathcal{K}$, the nearest point on the fitted surface was found by solving (4), and each was plotted against the corresponding data point in Figure 3. The GD between the data set and the fitted surface is 0.57, which is smaller than the total squared error reported for an augmentation of the Monod model in [20]. Overall we see in the error and figures that the SOC surface fits the data very well, and would therefore be adequate for use in optimization of this system.

5. Conclusion

We use the CCP to fit SOC constraints to data. Our main motivation is the microbial growth in bioprocesses, wherein certain standard growth rates like the Monod and Haldane functions lead to nonconvex constraints.

In numerical tests on both synthetic and experimental microbial growth data, we found that the fitted SOC surfaces achieved similar or better goodness of fit to standard techniques, and some robustness to noise. Most importantly, unlike most standard growth rates, the resulting SOC constraints are highly amenable to large-scale optimization [5, 14].

Future work includes systematically dealing with outliers and noise using stochastic and robust optimization, further analysis of local minima and the effect of various constraints on the SOC parameters, and fitting both SOC and semidefinite constraints to higher dimensional data, e.g., biochemical processes with multiple substrates and biomasses.

References

[1] M. Lobo, L. Vandenberghe, S. Boyd, H. Lebret, Applications of second-order cone programming, Linear Algebra and its Applications 284 (1998) 193–228.
[2] F. Alizadeh, D. Goldfarb, Second-order cone programming, Mathematical Programming 95 (2003) 3–51.
[3] J. Monod, The growth of bacterial cultures, Annual Review of Microbiology 3 (1) (1949) 371–394.
[4] D. Contois, Kinetics of bacterial growth: relationship between population density and specific growth rate of continuous cultures, Microbiology 21 (1) (1959) 40–50.
[5] J. Taylor, A. Rapaport, Second-order cone optimization of the gradostat, Computers & Chemical Engineering 151 (2021) 107347. doi:10.1016/j.compchemeng.2021.107347.
[6] A. L. Yuille, A. Rangarajan, The concave-convex procedure, Neural computation 15 (4) (2003) 915–936.
[7] T. Lipp, S. Boyd, Variations and extension of the convex–concave procedure, Optimization and Engineering 17 (2) (2016) 263–287.
[8] A. Fitzgibbon, M. Pilu, R. B. Fisher, Direct least square fitting of ellipses, IEEE Transactions on Pattern Analysis and Machine Intelligence 21 (5) (1999) 476–480.
[9] F. L. Bookstein, Fitting conic sections to scattered data, Computer graphics and image processing 9 (1) (1979) 56–71.
[10] A. Fitzgibbon, R. Fisher, A buyer's guide to conic fitting, in: Proceedings of the British Machine Vision Conference, 1995, pp. 51.1–51.10.
[11] P. Sturm, P. Gargallo, Conic fitting using the geometric distance, in: Asian Conference on Computer Vision, Springer, 2007, pp. 784–795.
[12] B. E. Rittmann, P. L. McCarty, Environmental biotechnology: principles and applications, McGraw-Hill Education, 2001.
[13] A. Mašić, S. Srinivasan, J. Billeter, D. Bonvin, K. Villez, Shape constrained splines as transparent black-box models for bioprocess modeling, Computers & Chemical Engineering 99 (2017) 96–105.
[14] J. A. Taylor, A. Rapaport, D. Dochain, Convex optimization of bioprocesses, Automatic Control, IEEE Transactions on (2022). doi:10.1109/TAC.2022.3167310.
[15] E. Krichen, A. Rapaport, E. Le Floc'h, E. Fouilland, A new kinetics model to predict the growth of micro-algae subjected to fluctuating availability of light, Algal Research 58 (2021) 102362.
[16] P. L. Rosin, A note on the least squares fitting of ellipses, Pattern Recognition Letters 14 (10) (1993) 799–808.

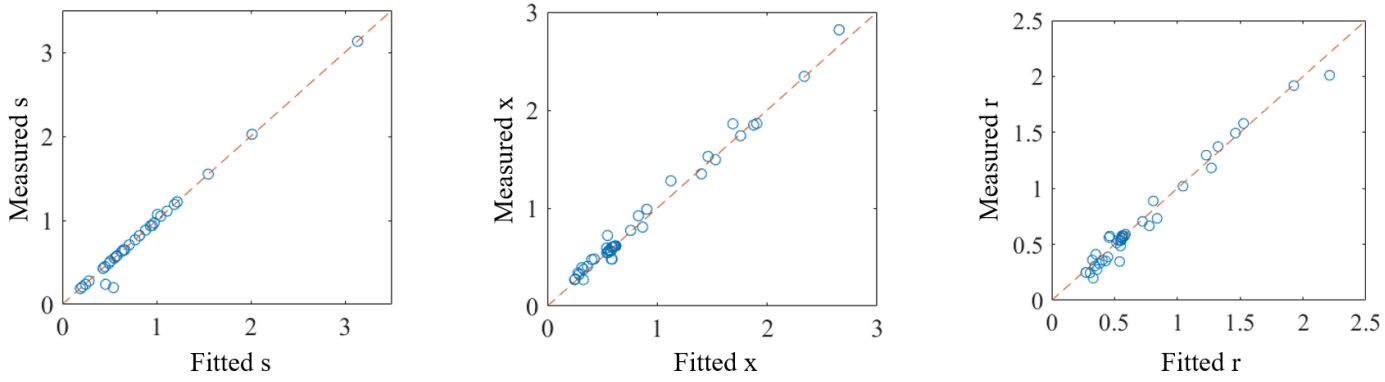

(a) (b) (c)

Figure 3: Measured versus fitted values, where the diagonal line corresponds to equality.

[17] F. Bach, R. Jenatton, J. Mairal, G. Obozinski, Optimization with sparsity-inducing penalties, Foundations and Trends® in Machine Learning 4 (1) (2012) 1–106.

[18] J. A. Taylor, A. Rapaport, D. Dochain, A sequential convex moving horizon estimator for bioprocesses, Journal of Process Control 116 (2022) 19–24. doi:10.1016/j.jprocont.2022.05.012.

[19] G. Bastin, D. Dochain, On-line estimation and adaptive control of bioreactors, Elsevier, 1990.

[20] E. Krichen, J. Harmand, M. Torrijos, J. Godon, N. Bernet, A. Rapaport, High biomass density promotes density-dependent microbial growth rate, Biochemical Engineering Journal 130 (2018) 66–75. doi:https://doi.org/10.1016/j.bej.2017.11.017.